Modeling the photo-induced inverse spin-Hall effect in Pt/semiconductor junctions

F. Bottegoni,[1, a)] C. Zucchetti,[1] G. Isella,[1] E. Pinotti,[1] M. Finazzi,[1] and F. Ciccacci[1]

Dipartimento di Fisica, Politecnico di Milano, Piazza Leonardo da Vinci 32, 20133 Milano, Italy

(Dated: 17 July 2018)

We show that the photon energy dependence of the photo-induced inverse spin-Hall effect (ISHE) signal at Pt/semiconductor junctions can be reproduced by a model that explicitly accounts for the electron spin diffusion length L_s in the semiconductor. In particular, we consider the Pt/GaAs, Pt/Ge and Pt/Si systems: although optical spin injection and transport of spin-polarized electrons in the conduction band of these semiconductors is ruled by different mechanisms, a simple one dimensional analytical diffusion model, where L_s is the free parameter, can reproduce the ISHE data in all cases. This highlights the potentialities of the photo-induced ISHE spectra as a tool to directly address fundamental spin transport properties in semiconductors.

[a)]Electronic mail: federico.bottegoni@polimi.it

In the past decades, semiconductors have turned out to be an ideal platform for the development of spintronic applications.[1] Pioneering studies on optical[2,3] and electrical[4–7] spin injection, transport[8,9] and dynamics[10,11] have been mainly performed in III-V semiconductors and related heterostructures.[12–17] However, in these semiconductors the lack of inversion symmetry introduces an efficent spin relaxation channel, represented by the Dyakonov-Perel mechanism,[18–20] which limits the electron spin lifetime to few nanoseconds at room temperature.[1]

An alternative platform for the development of spintronic devices is represented by group-IV semiconductors. In particular, much effort has been devoted to the study of spin generation and transport in Ge, Si and SiGe heterostructures, which are considered promising candidates in the field of spintronics thanks to the inversion symmetry, the integrability with nowadays electronic devices and the ability of suppressing hyperfine interactions.[21,22] The implementation of electrical spin injection/detection schemes in Ge[23–30] and Si[31–39] have paved the way to the understanding of the fundamental spin transport parameters in these materials, such as the electron spin diffusion length, the injected electron spin polarization and the spin-mixing conductance at the metal/semiconductor (SC) interface.

Notably, thanks to their large spin-orbit interaction (SOI), GaAs and Ge can be also exploited to electrically generate a pure spin current by means of the spin-Hall effect,[40–42] or to convert a spin current into a charge current through the inverse spin-Hall effect (ISHE),[26,29,43,44] whereas in Si the low SOI prevents efficient spin-to-charge interconversion phenomena.[45]

SOI plays a crucial role also for optical spin injection: in GaAs and Ge, the energy difference (Δ_{so} = 0.34 eV and 0.29 eV for GaAs and Ge, respectively) between heavy-hole (HH), light-hole (LH), and split-off (SO) states at the Γ point of the Brillouin zone allows generating a spin-oriented population of electrons in the conduction band. This is made possible by exploiting dipole selection rules for optical transitions with circularly-polarized light. In this case a maximum spin polarization $P = 50\%$ is achieved if the incident photon energy is tuned to the SC direct gap (E_d = 1.42 eV and 0.8 eV for GaAs and Ge, respectively, at room temperature).[2,3,46–49] Eventually, by applying strain or quantum confinement, the electron spin polarization can be enhanced well above 50%, as experimentally demonstrated both in GaAs[48,50] and Ge[51,52] based heterostructures.

A convenient spin detection scheme relies on ISHE, taking place in a thin Pt layer evapo-

rated on the top of the semiconductor,[53–58] where the optically-injected spin current is converted into a tranverse charge current through spin-dependent scattering with Pt nuclei.[53] The versatility of the optical spin injection technique also provides the possibility of designing non-local architectures, where spin is optically injected and electrically detected,[59] without the use of any ferromagnetic building block.

Unlike GaAs and Ge, Si has a very low spin-orbit interaction, being Δ_{so} only 40 meV. Nevertheless, it has been recently demonstrated, both theoretically[60] and experimentally,[61] that it is possible to optically inject a net spin polarization at the indirect gap of bulk Si (E_i = 1.1 eV at room temperature) with a maximum spin polarization $P \approx 5\%$, by exploiting phonon-assisted optical transitions with circularly-polarized light. Once more, the photogenerated spin current can be detected by exploiting the ISHE due to spin-oriented electrons injected into a thin Pt film acting as spin detector.[61]

In this paper we show that Pt/semiconductor junctions, where spin is optically injected and electrically detected, represent a valuable tool to estimate the electron spin diffusion length L_s in these materials. The photon energy dependence of the ISHE signal for GaAs, Ge and Si is interpreted in the frame of a one dimensional analytical diffusion model, where L_s is a free parameter, used to fit the corresponding dataset.

The investigated devices and the experimental geometry are sketched in Fig. 1a: a 5×5 mm^2-wide and 4 nm-thick Pt layer is deposited by e-beam evaporation on top of the SC substrate, namely a 350 μm-thick Si-doped GaAs(001) (doping concentration, $N_d = 2 \times 10^{18}$ cm^{-3}), a 450 μm-thick As-doped Ge(001) ($N_d = 1.6 \times 10^{16}$ cm^{-3}) and a 500 μm-thick P-doped Si(001) ($N_d = 8.95 \times 10^{14}$ cm^{-3}). Two 200 nm-thick Au/Ti contacts are then evaporated on each sample at the edges of the Pt layer along the y axis. The height of the Schottky barrier $E_B = 0.59$ eV, 0.63 and 0.83 eV for GaAs, Ge and Si, respectively, has been measured by fabricating metal-SC-metal junctions and exploiting the I-V curve analysis of Ref. 62.

In GaAs, optical spin orientation generates an electron spin population around Γ: spin-polarized hot electrons relax at the bottom of the conduction band and then diffuse towards the Pt layer (see Fig. 2b). In this case, both spin generation and transport occur at Γ. At variance from GaAs, in Ge optically-oriented spins are promoted in the conduction band around Γ and are scattered within hundreds of femtoseconds towards the four equivalent L minima, where spin transport takes place, partially preserving their initial spin polarization

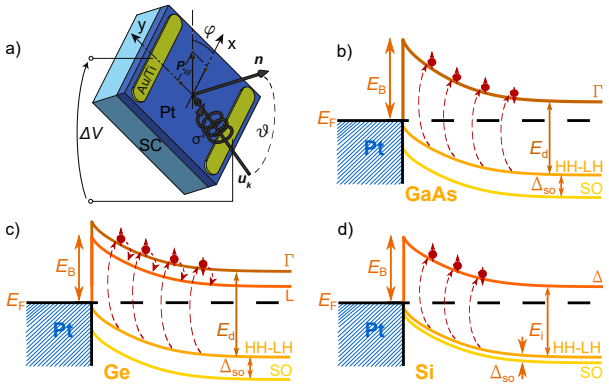

FIG. 1. (Color online) (a) Scheme of the Pt/SC (SC = GaAs, Ge, Si) sample and the experimental geometry: ϑ is the angle between the direction of the incident light (identified by the unit vector $\mathbf{u}_\mathrm{k}$) in the SC and the normal $\mathbf{n}$ to the sample surface, whereas φ is the angle between the projection of $\mathbf{u}_\mathrm{k}$ in the sample plane and the x axis. (b) Sketch of the band structure of the Pt/GaAs junction, where $E_\mathrm{B} = 0.59$ eV is the Schottky barrier height. Optically-oriented spins are generated in the GaAs conduction band from HH-LH states and diffuse around Γ. (c) Sketch of the band structure of the Pt/Ge junction ($E_\mathrm{B} = 0.63$ eV). Optically-oriented spins are generated in the Ge conduction band around Γ from HH-LH states and undergo an ultrafast $\Gamma - L$ scattering. (d) Sketch of the band structure of the Pt/Si junction ($E_\mathrm{B} = 0.83$ eV). Spin-polarized electrons are generated from HH and LH states and diffuse around the Δ-minima of the Si Brillouin zone.

(see Fig. 1c).[52] Finally, in Si optically-oriented spins are directly generated and diffuse along the Δ minima (see Fig. 1d), although the initial spin polarization, as already mentioned, is much smaller than in the case of GaAs and Ge.

ISHE measurements have been performed in air at room temperature: the light source consists of a supercontinuum laser, which provides a white broadband collimated beam with photon energies ranging from 0.7 to 1.75 eV. A monochromatic beam with a resolution of ≈ 10 meV is then generated by a dedicated optical setup and focused on the sample surface (spot size $d \approx 100$ μm) for optical spin injection. The circular polarization of the light is modulated by a photoelastic modulator (PEM) at 50 kHz. In our devices, spin accumulation is revealed in Pt since the spin current density $\mathbf{J}_\mathrm{s}$, diffusing along the z axis from the SC to the metal/SC interface, enters the Pt layer mainly through thermionic emission. In this case ISHE in Pt generates an electromotive field[63]

$$\mathbf{E}_\mathrm{ISHE} = D_\mathrm{ISHE}\mathbf{J}_\mathrm{s} \times \mathbf{u}_\mathrm{P}, \tag{1}$$

where D_{ISHE} is a parameter representing the efficiency of the ISHE process and $\mathbf{u}_{\mathrm{P}}$ is the unit vector corresponding to the direction of the spin polarization vector $\mathbf{P}$, parallel to the light wavevector inside the SC. We therefore measure the electromotive force $\Delta V \propto E_{\mathrm{ISHE}} \cdot d$ by a lock-in amplifier under open-circuit conditions between the two Au/Ti contacts. Due to the position of the electrical contacts (see Fig. 1a) and of the relative orientation between E_{ISHE} and $\mathbf{J}_{\mathrm{s}}$ expressed by Eq. 1, our experimental set-up is only sensitive to the x component of $\mathbf{P}$. Off normal illumination is achieved with the laser beam partially filling off-axis an achromatic plano-convex lens with 40 mm-focal length, which focuses the light on the sample with a polar angle $\vartheta \approx 10^{\circ}$ (see Fig. 1a), thus obtaining a polar angle $\vartheta_{\mathrm{SC}} \approx 2^{\circ}$ inside the SC. Eventually, the in-plane component of $\mathbf{P}$ can also be varied through the azimuthal angle φ, as shown in Fig. 1a.

The ISHE signal as a function of the incident photon energy for $\vartheta \approx 10^{\circ}$ and $\varphi = 0$ is shown in Fig. 2 for all the Pt/SC junctions. The experimental data have been normalized first to the photon flux Φ_{ph} inside the SC, simultaneously measuring the incident optical power on the sample and calculating the transmission coefficient through a multilayer optical analysis,[53,55,57,61] and then to the maximum value.

The behaviour of the signal for the Pt/GaAs junction (see Fig. 2a) indicates that, when the incident photon energy approaches the GaAs direct gap, i.e. $h\nu \approx 1.42$ eV, where the spin polarization is expected to be maximum, the ISHE signal is quite small. The latter increases only far from resonance conditions.[57] The same holds for the Pt/Si junction: indeed the ISHE signal is minimum at correspondence with photon energies approaching the Si indirect gap, i.e. $h\nu \approx 1.2$ eV, as shown in Fig.2c,[60] whereas it increases and reaches a plateau for $h\nu > 1.4$ eV. On the contrary, the energy dependence of the ISHE signal for the Pt/Ge junction (see Fig. 2b) resembles the one of the initial electron spin polarization,[64] as also confirmed by numerical calculations based on spin drift-diffusion equations.[57]

In order to capture the essential features of optically oriented spin transport in GaAs, Ge and Si, we consider an analytical model solving the diffusion equation in a semi-infinite bulk SC along the z axis. We neglect the current contributions given by the carrier-concentration gradient in the xy plane and we take into account the one dimensional spin transport problem along the z axis. Then, we set $z = 0$ at the sample surface so that $z \in [0, \infty]$. As a consequence of the optical spin injection, both spin-polarized electrons and holes are generated into the SC. However, since the electron spin lifetime is much larger than the hole spin

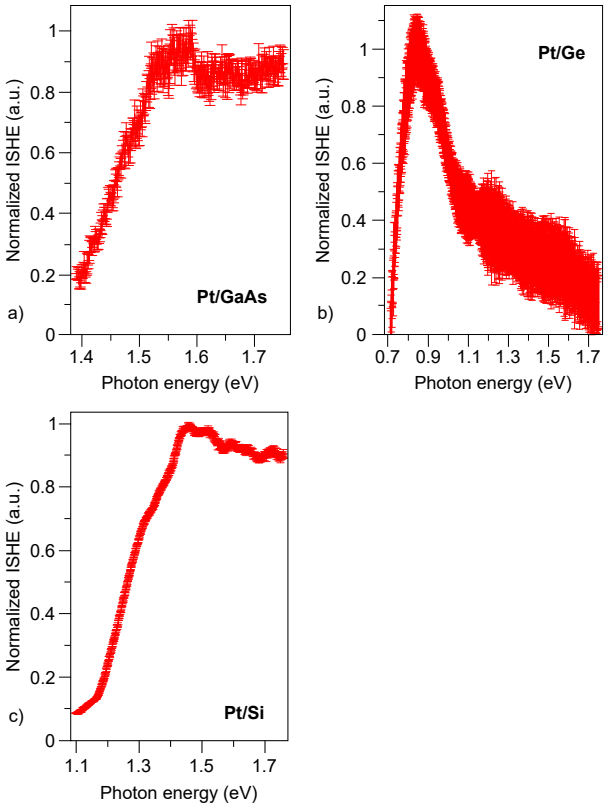

FIG. 2. (Color online) ISHE spectra for the Pt/GaAs (a), Pt/Ge (b) and Pt/Si (c) junctions, normalized first to the photon flux $\Phi_{\rm ph}$ inside the SC and then to the maximum value. Measurements have been performed at room temperature for $\vartheta \approx 10^{\circ}$ and $\varphi = 0$. Each data point represents the average value of five acquisitions and the bar length correspond to twice the associated standard deviation.

lifetime in GaAs,[10] Ge[65] and also Si,[33,37] we can assume that most of the spin signal is carried only by the spin polarized electrons, disregarding the contribution of the spin-polarized holes. In the pure diffusive regime and under steady-state conditions, we can write the following expression for the optically-induced electron spin density $s(z)$:

$$qD\left[\frac{\partial^2 s(z)}{\partial z^2} - \frac{s(z)}{L_{\rm s}^2}\right] = -G_0 e^{-\alpha z}, \tag{2}$$

being q the electron charge and D the ambipolar diffusion coefficient for the SC. The right-hand side of Eq. 2 represents the generation term in the optical spin injection process: $G_0 = qP_x\alpha\Phi_{\rm ph}$, where $\Phi_{\rm ph} = W/\pi d^2 h\nu$ is the photon flux. P_x represents the projection of the spin polarization along the x axis, α is the absorption coefficient and W is the optical power entering the SC. In this case, the spin current density in the SC can be

expressed as $J_s = -qD\,[\partial s(z)/\partial z]$. Since the spin diffusion length in Pt is of the order of few nanometers,[58,66] we solve Eq. 2 with the boundary conditions $s(0) = 0$, indicating that the spin density must vanish at the SC interface, and $s(\infty) = 0$, corresponding to a null spin density at the opposite edge of the sample. By solving Eq. 2, we find that the spin current density $J_s(0)$ at the SC interface, has the following expression

$$J_s(0) = q\Phi_{ph}\frac{P_x\alpha L_s}{1+\alpha L_s}. \tag{3}$$

The expression of Eq. 3 is similar to those already developed by Spicer[67,68] and Pierce *et al.*[69] to investigate photoconductivity measurements, photoemission and spin-polarized photoemission from bulk semiconductors. Recently, Sahasrabuddhe et al.[70] have presented a model for the electron emission yield $Y = J_s(0)/q\Phi_{ph}$, which takes into account finite emission (S_{em}) and recombination (S_{rec}) velocities at both front and back surfaces of the SC. Indeed, considering once again a semi-infinite SC and applying Eq. 2 with the boudary conditions $J_s(0) = q(S_{em} + S_{rec})s(0)$ and $J_s(\infty) = 0$, it is possible to show that the spin current density $J_s(0)$ at the SC interface is written as

$$J_s(0) = q\Phi_{ph}\frac{S_{em}}{S_{em}+S_{rec}+D/L_s}\frac{P_x\alpha L_s}{1+\alpha L_s}. \tag{4}$$

In semiconductors, typical values of S_{rec} are in the $10^0 - 10^3$ cm/s range, while D is of the order of $10 - 100$ cm^2/s.[71] Thus, for $L_s \approx 1$ μm we get $D/L_s \approx 10^5$ cm/s. Being $D/L_s \gg S_{rec}, S_{em}$, Eq. 4 becomes

$$J_s(0) = q\Phi_{ph}\delta\frac{P_x\alpha L_s}{1+\alpha L_s} \tag{5}$$

which yields the same photon energy dependence of Eq. 3, multiplied by the prefactor $\delta = S_{em}L_s/D$. As a function of the S_{em} value, which accounts for the fraction of electrons overcoming the Schottky barrier and being transferred from SC to the Pt layer, the absolute value of $J_s(0)$ predicted from Eq. 5 can be significantly lower than the one obtained from Eq. 3, where the effects of the Schottky barrier are not taken into account. However, since Eqs. 3 and 5 are exploited in the present case only to explain the photon energy dependence of the ISHE signal, the issues related to the absolute value of the ISHE signal will not be considered in the following.

Since, from Eq. 1, $J_s(0) \propto \Delta V$, Eqs. 3 and 5 can be used to evaluate the dependence of the ISHE signal as a function of the incident photon energy, once that $P(h\nu)$ and $\alpha(h\nu)$

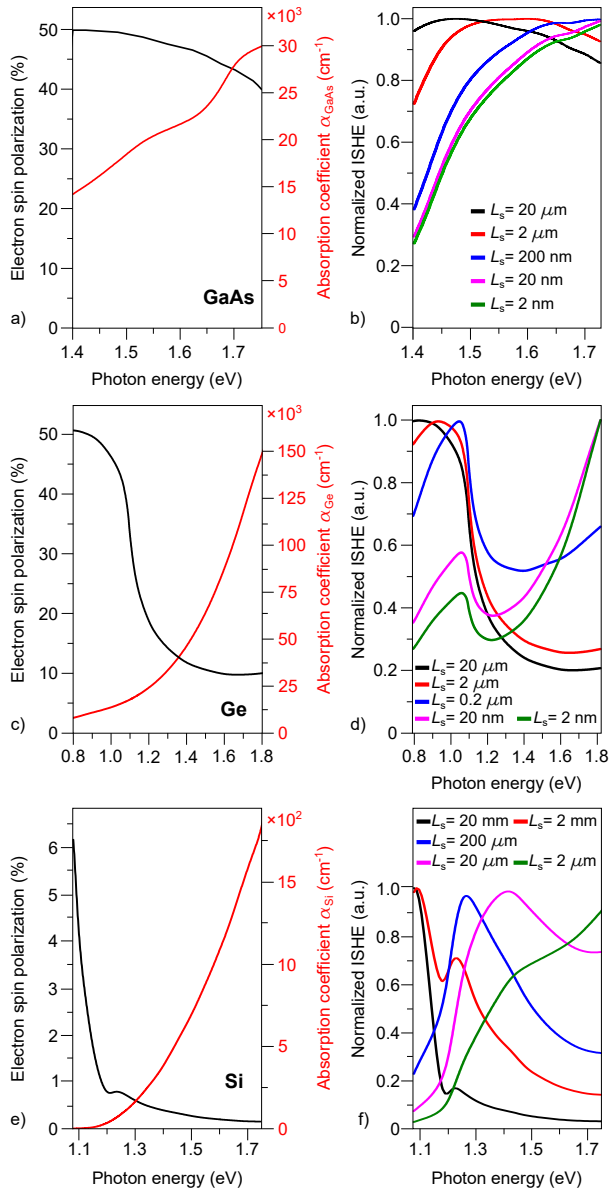

FIG. 3. (Color online) Photon energy dependence of the electron spin polarization (black curve) and absorption coefficient (red curve) of GaAs (a) from Refs. 72 and 73, Ge (c) from Refs. 64 and 74, and Si (e) from Ref. 60. (b) Photon energy dependence of the normalized ISHE signal for the Pt/GaAs (b), Pt/Ge (d), and Pt/Si (f) junctions, calculated from Eq. 3 with the P_x and α values displayed in panel (a), (c) and (e), respectively, for different electron spin diffusion lengths.

are known. Fig. 3 (left column) shows the initial electron spin polarization $P(h\nu)$ and the absorption coefficient $\alpha(h\nu)$ for all the investigated junctions (data are taken from Refs. 72 and 73 for GaAs, from Refs. 64 and 74 for Ge and from Ref. 60 for Si). Fig. 3 (right column) also displays the corresponding normalized ISHE signal ΔV, evaluated from Eq. 3,

for different L_s values.

For all the junctions, the model suggests that, upon increasing L_s, the energy dependence of the ISHE signal goes from a "Ge-like"trend, reminiscent of the initial electron spin polarization, to a "Si-like"trend, where the maximum ΔV is obtained when the incident photon energy is far from the corresponding SC absorption edge.

Eventually, Eq. 3 can also be exploited to fit the experimental data of Fig. 2, by considering L_s as a free parameter. The best interpolation is obtained for $L_s = 30 \pm 5$ nm and $L_s = 9 \pm 2$ μm for GaAs and Si, respectively. These results can be explained by considering that the outcome of Eq. 3 basically depends on the interplay between the absorption length $\ell_\alpha = 1/\alpha$ and the spin diffusion length L_s in the SC. In GaAs and Si the absorption coefficient is such that $\ell_\alpha \gg L_s$ for incident photon energies close to the direct (indirect) GaAs (Si) gap (see Figs. 3a and 3e for GaAs and Si, respectively). Thus, most of the photo-electrons are generated at a distance from the Pt/SC interface much larger than L_s. This results in a strongly depolarized photoelectron current and in a very small signal. As $h\nu$ is increased, ℓ_α approaches L_s. In this case, despite the initial electron spin polarization is smaller, all the photogenerated electrons enter the Pt layer before depolarizing and the ISHE signal becomes larger.

At variance from GaAs and Si, for Ge the sensitivity of the model does not allow yielding a precise estimation of L_s. Indeed, as shown in Fig. 3d, for L_s values comparable to or larger than 1 μm, Eq. 3 provides a similar outcome, so that $L_s \approx 1$ μm represents only a lower bound estimation of the spin diffusion length in Ge. This results from the fact that $\ell_\alpha \leq L_s$ in all the investigated energy range (see Fig. 3c): as a consequence, all the photogenerated spins enter the Pt layer before depolarizing and the energy dependence of the ISHE signal is only dictated by the initial electron spin polarization P_x. It is also interesting to note that Eq. 3 assumes that the initial spin polarization in the Ge conduction band is completely preserved at the L minima, which can be considered a reasonable assumption since, although spin-polarized electrons are generated around the Γ point of the Brillouin zone, the $\Gamma - L$ scattering occurs in a timescale much lower than the spin lifetime ($\tau_s = L_s^2/D_{Ge} \approx 10^{-9}$ s). The results of the fitting procedure for all the investigated junctions are shown in Fig. 4a and 4c together with the corresponding dataset for GaAs and Si, respectively, whereas a representative fitting curve for $L_s = 10$ μm is shown in Fig. 4b for Ge. The estimated L_s values are in agreement with those previously reported in the literature for GaAs,[6,44]

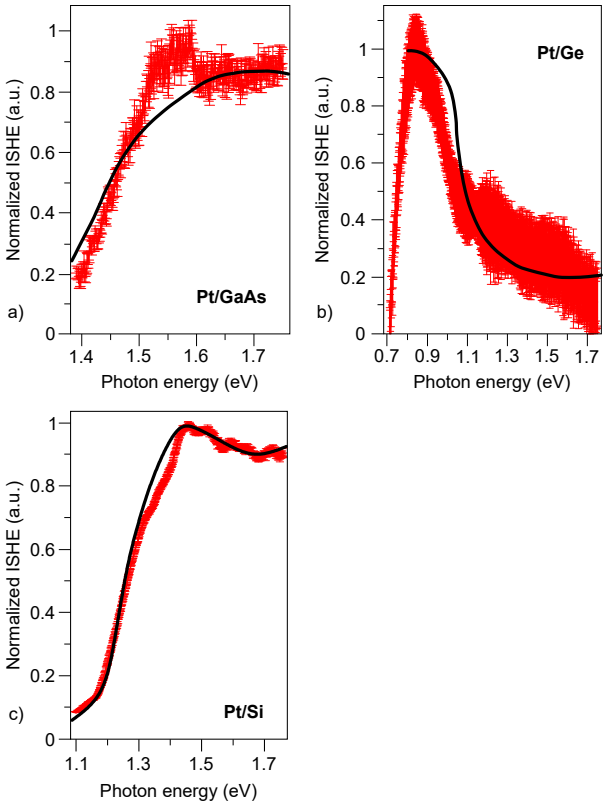

FIG. 4. (Color online) Experimental (red line) photon energy dependence of the normalized photoinduced ISHE signal for the Pt/GaAs (a), Pt/Ge (b) and Pt/Si (c) junctions. The black curves represent the best fit obtained from Eq. 3, which yields an electron spin diffusion length $L_s = 30 \pm 5$ nm and μm and $L_s = 9 \pm 2$ μm for GaAs and Si, respectively. For Ge, the black curve represents the result of Eq. 3 for $L_s = 10$ μm.

Ge[29,55,57,75] and Si[76–78], indicating that optical ISHE spectra can be used as a practical tool to estimate the spin diffusion length in semiconductors.

Note that Eqs. 3 and 5 are valid only when the electron dynamics is determined only by diffusion and no drift currents are present. Although the built-in electric field associated with the Schottky barrier might affect electron transport across the Pt/SC junction, the comparison with the numerical results of Ref. 57, obtained within a model encompassing drift and diffusion, shows that the principal role is played by the latter.

Finally, it is important to point out that Eq. 3 reproduces the photon energy dependence of the ISHE signal for an optically-oriented spin population, that is fully relaxed at the bottom of the conduction band but preserves the initial spin polarization value. This is a valid assumption for incident photon energies close to the SC gap, especially for GaAs

and Si, where optical spin generation and transport occur in the same valley. However, for energies much larger than the SC gap, scattering with phonons may drastically alter the spin polarization profile under steady-state conditions,[79] so that the proper spin-relaxation cross sections for hot electrons as a function of the incident photon energy should be taken into account.

In conclusion, we have demonstrated that a simple one dimensional model accounting for photon absorption and electron diffusion allows reproducing the photon energy dependence of the ISHE signal at Pt/GaAs, Pt/Ge and Pt/Si junctions. This can be exploited to estimate the electron spin diffusion length in semiconductors and highlights the potentialities of ISHE measurements as spectroscopic tool for the investigation of fundamental spin transport properties in semiconductors.

REFERENCES

[1]I. Zutić, J. Fabian, and S. Das Sarma, "Spintronics: Fundamentals and applications," Rev. Mod. Phys. **76**, 323–410 (2004).

[2]D. Pierce and F. Meier, "Photoemission of spin-polarized electrons from GaAs," Phys. Rev. B **13**, 5484 (1976).

[3]H.-J. Drouhin, C. Hermann, and G. Lampel, "Photoemission from activated gallium arsenide. II. Spin polarization versus kinetic energy analysis," Phys. Rev. B **31**, 3872 (1985).

[4]A. T. Hanbicki, O. M. J. van 't Erve, R. Magno, G. Kioseoglou, C. H. Li, B. T. Jonker, G. Itskos, R. Mallory, M. Yasar, and A. Petrou, "Analysis of the transport process providing spin injection through an Fe/AlGaAs Schottky barrier," Appl. Phys. Lett. **82**, 4092 (2003).

[5]B. T. Jonker, G. Kioseoglou, A. T. Hanbicki, C. H. Li, and P. E. Thompson, "Electrical spin-injection into silicon from a ferromagnetic metal/tunnel barrier contact," Nat. Phys. **3**, 542 (2007).

[6]M. Tran, H. Jaffrès, C. Deranlot, J.-M. George, A. Fert, A. Miard, and A. Lemaître, "Enhancement of the Spin Accumulation at the Interface between a Spin-Polarized Tunnel Junction and a Semiconductor," Phys. Rev. Lett. **102**, 036601 (2009).

[7]J. Sinova, S. O. Valenzuela, J. Wunderlich, C. H. Back, and T. Jungwirth, "Spin Hall

effects," Rev. Mod. Phys. **87**, 1213 (2015).

[8]Y. Kato, R. C. Myers, a. C. Gossard, and D. D. Awschalom, "Coherent spin manipulation without magnetic fields in strained semiconductors." Nature **427**, 50 (2004).

[9]S. A. Crooker, M. Furis, X. Lou, C. Adelmann, D. L. Smith, C. J. Palmstrøm, and P. A. Crowell, "Imaging spin transport in lateral ferromagnet/semiconductor structures." Science **309**, 2191 (2005).

[10]J. Kikkawa and D. Awschalom, "Resonant Spin Amplification in n-Type GaAs," Phys. Rev. Lett. **80**, 4313 (1998).

[11]M. Wu, J. Jiang, and M. Weng, "Spin dynamics in semiconductors," Phys. Rep. **493**, 61 (2010).

[12]R. C. Miller, D. A. Kleinman, W. A. Nordland, Jr., and A. C. Gossard, "Luminescence studies of optically pumped quantum wells in GaAs-$Al_xGa_{1-x}As$ multilayer structures," Phys. Rev. B **22**, 863 (1980).

[13]S. F. Alvarado, F. Ciccacci, and M. Campagna, "GaAs-$Al_xGa_{1-x}As$ superlattices as sources of polarized photoelectons," Appl. Phys. Lett. **39**, 615 (1981).

[14]F. Ciccacci, H.-J. Drouhin, C. Hermann, R. Houdre, and G. Lampel, "Spin-polarized photoemission from AlGaAs/GaAs heterojunction: A convenient highly polarized electron source," Appl. Phys. Lett. **54**, 632 (1989).

[15]H. C. Koo, J. H. Kwon, J. Eom, J. Chang, S. H. Han, and M. Johnson, "Control of spin precession in a spin-injected field effect transistor." Science **325**, 1515 (2009).

[16]R. Mattana, J.-M. George, H. Jaffrès, F. Nguyen Van Dau, A. Fert, B. Lépine, A. Guivarc'h, and G. Jézéquel, "Electrical Detection of Spin Accumulation in a p-Type GaAs Quantum Well," Phys. Rev. Lett. **90**, 166601 (2003).

[17]G. Wang, B. L. Liu, A. Balocchi, P. Renucci, C. R. Zhu, T. Amand, C. Fontaine, and X. Marie, "Gate control of the electron spin-diffusion length in semiconductor quantum wells." Nat. Commun. **4**, 2372 (2013).

[18]F. Meier and B. P. Zakharchenya, eds., *Optical orientation (Modern Problems in Condensed Matter Sciences, Vol. 8)* (Elsevier, Amsterdam, 1984).

[19]F. Bottegoni, H.-J. Drouhin, G. Fishman, and J.-E. Wegrowe, "Probability- and spin-current operators for effective Hamiltonians," Phys. Rev. B **85**, 235313 (2012).

[20]F. Bottegoni, H.-J. Drouhin, J.-E. Wegrowe, and G. Fishman, "Probability-current definition in presence of spin-orbit interaction," J. Appl. Phys. **111**, 07C305 (2012).

[21]B. E. Kane, "A silicon-based nuclear spin quantum computer," Nature **393**, 133 (1998).

[22]P. S. Fodor and J. Levy, "Group IV solid state proposals for quantum computation," J. Phys. Condens. Matter **18**, S745 (2006).

[23]C. Shen, T. Trypiniotis, K. Y. Lee, S. N. Holmes, R. Mansell, M. Husain, V. Shah, X. V. Li, H. Kurebayashi, I. Farrer, C. H. de Groot, D. R. Leadley, G. Bell, E. H. C. Parker, T. Whall, D. A. Ritchie, and C. H. W. Barnes, "Spin transport in germanium at room temperature," Appl. Phys. Lett. **97**, 162104 (2010).

[24]A. Jain, L. Louahadj, J. Peiro, J. C. Le Breton, C. Vergnaud, A. Barski, C. Beigné, L. Notin, A. Marty, V. Baltz, S. Auffret, E. Augendre, H. Jaffrs, J. M. George, and M. Jamet, "Electrical spin injection and detection at Al_2O_3/n-type germanium interface using three terminal geometry," Appl. Phys. Lett. **99**, 162102 (2011).

[25]A. Jain, J.-C. Rojas-Sanchez, M. Cubukcu, J. Peiro, J. Le Breton, E. Prestat, C. Vergnaud, L. Louahadj, C. Portemont, C. Ducruet, V. Baltz, A. Barski, P. Bayle-Guillemaud, L. Vila, J.-P. Attané, E. Augendre, G. Desfonds, S. Gambarelli, H. Jaffrès, J.-M. George, and M. Jamet, "Crossover from Spin Accumulation into Interface States to Spin Injection in the Germanium Conduction Band," Phys. Rev. Lett. **109**, 106603 (2012).

[26]J.-C. Rojas-Sánchez, M. Cubukcu, A. Jain, C. Vergnaud, C. Portemont, C. Ducruet, A. Barski, A. Marty, L. Vila, J.-P. Attané, E. Augendre, G. Desfonds, S. Gambarelli, H. Jaffrès, J.-M. George, and M. Jamet, "Spin pumping and inverse spin Hall effect in germanium," Phys. Rev. B **88**, 064403 (2013).

[27]S. Dushenko, M. Koike, Y. Ando, T. Shinjo, M. Myronov, and M. Shiraishi, "Experimental Demonstration of Room-Temperature Spin Transport in n-Type Germanium Epilayers," Phys. Rev. Lett. **114**, 196602 (2015).

[28]F. Rortais, S. Oyarzún, F. Bottegoni, J.-C. Rojas-Sánchez, P. Laczkowski, A. Ferrari, C. Vergnaud, C. Ducruet, C. Beigné, N. Reyren, A. Marty, J.-P. Attané, L. Vila, S. Gambarelli, J. Widiez, F. Ciccacci, H. Jaffrès, J.-M. George, and M. Jamet, "Spin transport in p -type germanium," J. Phys. Condens. Matter **28**, 165801 (2016).

[29]S. Oyarzún, F. Rortais, J.-C. Rojas-Sánchez, F. Bottegoni, P. Laczkowski, C. Vergnaud, S. Pouget, H. Okuno, L. Vila, J.-P. Attané, C. Beigné, A. Marty, S. Gambarelli, C. Ducruet, J. Widiez, J.-M. George, H. Jaffrès, and M. Jamet, "Spin-Charge Conversion Phenomena in Germanium," J. Phys. Soc. Japan **86**, 011002 (2017).

[30]F. Rortais, C. Vergnaud, A. Marty, L. Vila, J.-P. Attané, J. Widiez, C. Zucchetti, F. Bot-

tegoni, H. Jaffrès, J.-M. George, and M. Jamet, "Non-local electrical spin injection and detection in germanium at room temperature," Appl. Phys. Lett. **111**, 182401 (2017).

[31]O. M. J. van 't Erve, A. T. Hanbicki, M. Holub, C. H. Li, C. Awo-Affouda, P. E. Thompson, and B. T. Jonker, "Electrical injection and detection of spin-polarized carriers in silicon in a lateral transport geometry," Appl. Phys. Lett. **91**, 212109 (2007).

[32]G. Kioseoglou, A. T. Hanbicki, R. Goswami, O. M. J. van 't Erve, C. H. Li, G. Spanos, P. E. Thompson, and B. T. Jonker, "Electrical spin injection into Si: A comparison between Fe/Si Schottky and Fe/Al_2O_3 tunnel contacts," Appl. Phys. Lett. **94**, 122106 (2009).

[33]S. P. Dash, S. Sharma, R. S. Patel, M. P. de Jong, and R. Jansen, "Electrical creation of spin polarization in silicon at room temperature." Nature **462**, 491 (2009).

[34]J. Li and I. Appelbaum, "Lateral spin transport through bulk silicon," Appl. Phys. Lett. **100**, 162408 (2012).

[35]R. Jansen, "Silicon spintronics," Nat. Mater. **11**, 400 (2012).

[36]A. Dankert, R. S. Dulal, and S. P. Dash, "Efficient Spin Injection into Silicon and the Role of the Schottky Barrier," Sci. Rep. **3**, 3196 (2013).

[37]E. Shikoh, K. Ando, K. Kubo, E. Saitoh, T. Shinjo, and M. Shiraishi, "Spin-Pump-Induced Spin Transport in p-Type Si at Room Temperature," Phys. Rev. Lett. **110**, 127201 (2013).

[38]R. Jansen, A. Spiesser, H. Saito, and S. Yuasa, "Nonlinear spin transport in a rectifying ferromagnet/semiconductor Schottky contact," Phys. Rev. B **92**, 075304 (2015).

[39]T. Sasaki, Y. Ando, M. Kameno, T. Tahara, H. Koike, T. Oikawa, T. Suzuki, and M. Shiraishi, "Spin Transport in Nondegenerate Si with a Spin MOSFET Structure at Room Temperature," Phys. Rev. Appl. **2**, 034005 (2014).

[40]Y. K. Kato, R. C. Myers, A. C. Gossard, and D. D. Awschalom, "Observation of the spin Hall effect in semiconductors." Science **306**, 1910 (2004).

[41]S. Matsuzaka, Y. Ohno, and H. Ohno, "Electron density dependence of the spin Hall effect in GaAs probed by scanning Kerr rotation microscopy," Phys. Rev. B **80**, 241305 (2009).

[42]F. Bottegoni, C. Zucchetti, S. Dal Conte, J. Frigerio, E. Carpene, C. Vergnaud, M. Jamet, G. Isella, F. Ciccacci, G. Cerullo, and M. Finazzi, "Spin-Hall Voltage over a Large Length Scale in Bulk Germanium," Phys. Rev. Lett. **118**, 167402 (2017).

[43]K. Ando, S. Takahashi, J. Ieda, H. Kurebayashi, T. Trypiniotis, C. H. W. Barnes, S. Maekawa, and E. Saitoh, "Electrically tunable spin injector free from the impedance

mismatch problem," Nat. Mater. **10**, 655 (2011).

[44]F. Bottegoni, A. Ferrari, G. Isella, M. Finazzi, and F. Ciccacci, "Experimental evaluation of the spin-Hall conductivity in Si-doped GaAs," Phys. Rev. B **88**, 121201 (2013).

[45]K. Ando and E. Saitoh, "Observation of the inverse spin Hall effect in silicon." Nat. Commun. **3**, 629 (2012).

[46]R. Allenspach, F. Meier, and D. Pescia, "Experimental Symmetry Analysis of Electronic States by Spin-Dependent Photoemission," Phys. Rev. Lett. **51**, 2148 (1983).

[47]F. Bottegoni, G. Isella, S. Cecchi, and F. Ciccacci, "Spin polarized photoemission from strained Ge epilayers," Appl. Phys. Lett. **98**, 242107 (2011).

[48]F. Bottegoni, A. Ferrari, G. Isella, S. Cecchi, M. Marcon, D. Chrastina, G. Trezzi, and F. Ciccacci, "Ge/SiGe heterostructures as emitters of polarized electrons," J. Appl. Phys. **111**, 063916 (2012).

[49]F. Bottegoni, A. Ferrari, G. Isella, M. Finazzi, and F. Ciccacci, "Enhanced orbital mixing in the valence band of strained germanium," Phys. Rev. B **85**, 245312 (2012).

[50]Y. A. Mamaev, L. G. Gerchikov, Y. P. Yashin, D. A. Vasiliev, V. V. Kuzmichev, V. M. Ustinov, A. E. Zhukov, V. S. Mikhrin, and A. P. Vasiliev, "Optimized photocathode for spin-polarized electron sources," Appl. Phys. Lett. **93**, 081114 (2008).

[51]A. Ferrari, F. Bottegoni, G. Isella, S. Cecchi, and F. Ciccacci, "Epitaxial $Si_{1-x}Ge_x$ alloys studied by spin-polarized photoemission," Phys. Rev. B **88**, 115209 (2013).

[52]F. Pezzoli, F. Bottegoni, D. Trivedi, F. Ciccacci, A. Giorgioni, P. Li, S. Cecchi, E. Grilli, Y. Song, M. Guzzi, H. Dery, and G. Isella, "Optical Spin Injection and Spin Lifetime in Ge Heterostructures," Phys. Rev. Lett. **108**, 156603 (2012).

[53]K. Ando, M. Morikawa, T. Trypiniotis, Y. Fujikawa, C. H. W. Barnes, and E. Saitoh, "Photoinduced inverse spin-Hall effect: Conversion of light-polarization information into electric voltage," Appl. Phys. Lett. **96**, 082502 (2010).

[54]K. Ando, M. Morikawa, T. Trypiniotis, Y. Fujikawa, C. H. W. Barnes, and E. Saitoh, "Direct conversion of light-polarization information into electric voltage using photoinduced inverse spin-Hall effect in Pt/GaAs hybrid structure: Spin photodetector," J. Appl. Phys. **107**, 113902 (2010).

[55]F. Bottegoni, A. Ferrari, S. Cecchi, M. Finazzi, F. Ciccacci, and G. Isella, "Photoinduced inverse spin Hall effect in Pt/Ge(001) at room temperature," Appl. Phys. Lett. **102**, 152411 (2013).

[56]F. Bottegoni, M. Celebrano, M. Bollani, P. Biagioni, G. Isella, F. Ciccacci, and M. Finazzi, "Spin voltage generation through optical excitation of complementary spin populations." Nat. Mater. **13**, 790 (2014).

[57]G. Isella, F. Bottegoni, A. Ferrari, M. Finazzi, F. Ciccacci, "Photon energy dependence of photo-induced inverse spin-Hall effect in Pt / GaAs and Pt / Ge," Appl. Phys. Lett. **106**, 232402 (2015).

[58]F. Bottegoni, A. Ferrari, F. Rortais, C. Vergnaud, A. Marty, G. Isella, M. Finazzi, M. Jamet, and F. Ciccacci, "Spin diffusion in Pt as probed by optically generated spin currents," Phys. Rev. B **92**, 214403 (2015).

[59]C. Zucchetti, F. Bottegoni, C. Vergnaud, F. Ciccacci, G. Isella, L. Ghirardini, M. Celebrano, F. Rortais, A. Ferrari, A. Marty, M. Finazzi, and M. Jamet, "Imaging spin diffusion in germanium at room temperature," Phys. Rev. B **96**, 014403 (2017).

[60]J. L. Cheng, J. Rioux, J. Fabian, and J. E. Sipe, "Theory of optical spin orientation in silicon," Phys. Rev. B **83**, 165211 (2011).

[61]F. Bottegoni, C. Zucchetti, F. Ciccacci, M. Finazzi, and G. Isella, "Optical generation of pure spin currents at the indirect gap of bulk Si," Appl. Phys. Lett. **110**, 042403 (2017).

[62]R. Nouchi, "Extraction of the Schottky parameters in metal-semiconductor-metal diodes from a single current-voltage measurement," J. Appl. Phys. **116**, 184505 (2014).

[63]E. Saitoh, M. Ueda, H. Miyajima, and G. Tatara, "Conversion of spin current into charge current at room temperature: Inverse spin-Hall effect," Appl. Phys. Lett. **88**, 182509 (2006).

[64]J. Rioux and J. E. Sipe, "Optical injection and control in germanium: Thirty-band kp theory," Phys. Rev. B **81**, 155215 (2010).

[65]C. Guite and V. Venkataraman, "Temperature dependence of spin lifetime of conduction electrons in bulk germanium," Appl. Phys. Lett. **101**, 252404 (2012).

[66]M. Isasa, E. Villamor, L. E. Hueso, M. Gradhand, and F. Casanova, "Temperature dependence of spin diffusion length and spin Hall angle in Au and Pt," Phys. Rev. B **91**, 024402 (2015).

[67]W. E. Spicer, "Photoemissive, Photoconductive, and Optical Absorption Studies of Alkali-Antimony Compounds",Phys. Rev. **112**, 114 (1958).

[68]W. E. Spicer, "Negative affinity 3-5 photocathodes: Their physics and technology," Appl. Phys. **12**, 115 (1977).

[69]D. T. Pierce, R. J. Celotta, G.-G. Wang, W. N. Unerti, A. Galejs, C. E. Kuyatt, and S. R. Mielczarek, "GaAs spin polarized electron source," Rev. Sci. Instrum. **51**, 478 (1980).

[70]K. Sahasrabuddhe, J. W. Schwede, I. Bargatin, J. Jean, R. T. Howe, Z.-X. Shen, and N. A. Melosh, "A model for emission yield from planar photocathodes based on photon-enhanced thermionic emission or negative-electron-affinity photoemission," Rev. Sci. Instrum. **51**, 478 (1980).

[71]E. Yablonovitch, D. L. Allara, C. C. Chang, T. Gmitter, and T. B. Bright, "Unusually Low Surface-Recombination Velocity on Silicon and Germanium Surfaces," Phys. Rev. Lett. **57**, 249 (1986).

[72]F. Nastos, J. Rioux, M. Strimas-Mackey, B. Mendoza, and J. Sipe, "Full band structure LDA and k·p calculations of optical spin-injection," Phys. Rev. B **76**, 205113 (2007).

[73]M. D. Sturge, "Optical Absorption of Gallium Arsenide between 0.6 and 2.75 eV," Phys. Rev. **127**, 768 (1962).

[74]H. Philipp and E. Taft, "Optical Constants of Germanium in the Region 1 to 10 eV," Phys. Rev. **113**, 1002 (1959).

[75]P. Li, Y. Song, and H. Dery, "Intrinsic spin lifetime of conduction electrons in germanium," Phys. Rev. B **86**, 085202 (2012).

[76]J. L. Cheng, M. W. Wu, and J. Fabian, "Theory of the Spin Relaxation of Conduction Electrons in Silicon," Phys. Rev. Lett. **104**, 016601 (2010).

[77]P. Li and H. Dery, "Spin-Orbit Symmetries of Conduction Electrons in Silicon," Phys. Rev. Lett. **107**, 107203 (2011).

[78]Y. Song and H. Dery, "Analysis of phonon-induced spin relaxation processes in silicon," Phys. Rev. B **86**, 085201 (2012).

[79]C. Zucchetti, F. Bottegoni, G. Isella, M. Finazzi, F. Rortais, C. Vergnaud, J. Widiez, M. Jamet, and F. Ciccacci, "Spin-to-charge conversion for hot photoexcited electrons in germanium," Phys. Rev. B **97**, 125203 (2018).